

Structural Studies on the Combining Site of the Myeloma Protein MOPC 315

Raymond A. DWEK, Johanna C. A. KNOTT, Derek MARSH, Alan C. McLAUGHLIN, Elizabeth M. PRESS, Nicholas C. PRICE, and Alastair I. WHITE

Department of Biochemistry, University of Oxford

(Received June 25/December 9, 1974)

1. Analysis of the electron spin resonance spectra of different spin-labelled haptens when bound to the Fv fragment from the immunoglobulin A of the mouse myeloma protein MOPC 315 suggests that the combining site is a cleft of overall dimension $11 \text{ \AA} \times 9 \text{ \AA} \times 6 \text{ \AA}$ which has considerable structural rigidity.

2. The 270 MHz proton nuclear magnetic resonance spectrum of the amino acid residues in and around the combining site is obtained by use of paramagnetic difference spectroscopy involving a spin-labelled hapten. There are only the equivalent of about 30 aliphatic and 30 aromatic protons in this difference spectrum.

3. The C-2 and C-4 proton resonances of three histidine residues in the Fv fragment are observed to titrate with pH. The pK_a values of these histidine residues are about 8.1, 6.9 and 6.1. The resonances of the histidine residue with pK_a value 8.1 show anomalous behaviour in splitting into two or more components. The values of the chemical shifts of the C-2 and C-4 protons alter slightly in the presence of hapten, particularly for the histidine residues with pK_a values of 6.9 and 6.1. The resonances of these two residues are not observable in the presence of the spin-labelled hapten indicating that these two histidines are in the region of the combining site.

4. The existence of lanthanide binding sites of the Fv fragment, an essential prerequisite in mapping studies, has been demonstrated by measurements of the solvent water relaxation rates in Gd^{3+} solutions.

The problem of recognition in solution is a general one throughout biology, of which the recognition by antibodies of antigenic determinants is a particularly important example. An antibody directed against an antigenic determinant of a given molecule will react only with this determinant or another very similar structure. This specificity must result from the three-dimensional complementarity of the antibody combining site and the antigenic determinant.

Conventionally, problems involving three-dimensional structure are attempted using X-ray crystallographic techniques. However the only technique which can give structural information in solution (in principle comparable to that obtainable from X-ray work) is nuclear magnetic resonance (NMR).

Abbreviations. IgA, immunoglobulin A; Fab' fragment, N-terminal half of heavy chain and the whole of the light chain; Fv fragment, variable region of heavy and light chain; NMR, nuclear magnetic resonance; ESR, electron spin resonance.

For structural studies it is obviously desirable to work with homogeneous antibodies, but nearly all conventionally raised antibodies are heterogeneous populations of immunoglobulins. However in certain forms of cancer of immunoglobulin-synthesising cells (known as myelomatosis) homogeneous immunoglobulin molecules (known as myeloma proteins) are produced. These proteins have been shown by their ligand-binding properties and many immunochemical parameters to resemble antibodies.

By comparison with X-ray work, NMR three-dimensional structural determination is in its infancy and the problems of sensitivity, resolution and assignment are still very major ones. The most ambitious NMR structural determination of a protein so far is that of lysozyme (molecular weight ≈ 14000) and here considerable success has already been achieved [1], although much of the initial work was helped by the X-ray structure. The problem of structural deter-

mination by NMR and X-ray methods becomes increasingly complex as the size of the molecule increases. The smallest antibody fragment that preserves the integrity of the combining site is the Fv fragment of protein MOPC 315 [2]. This has a molecular weight of 25000 nearly twice that of lysozyme, and attempts to obtain suitable crystals of the Fv fragment for X-ray studies have so far been unsuccessful. In fact there have been few X-ray structures below about 4.5 Å resolution reported. The papers by Poljak *et al.* [3] on the 2.8 Å resolution of a human myeloma immunoglobulin fragment Fab New (molecular weight 50000); by Amzel *et al.* [4] on the 3.5 Å map with the γ -hydroxy derivative of vitamin K, in the combining site of Fab New; by Schiffer *et al.* [5] on the 3.5 Å map of a human lambda-type Bence-Jones dimer (molecular weight 46000); by Epp *et al.* [6] on the 2.8 Å map of the variable region of a human kappa-type Bence-Jones dimer (molecular weight 22000) and by Padlan *et al.* [7] on the 4.5 Å map of the Fab fragment (molecular weight 50000) from the phosphorylcholine binding McPC 603, provide a key to the previous literature.

In much the same way as X-ray crystallographic structural studies of proteins initially require heavy atoms as reference points, so the corresponding NMR studies require paramagnetic centres [8]. Often these are metal ions such as those of the La^{3+} ions, Mn^{2+} and Co^{2+} , but sometimes spin-label probes can be used [8].

We have begun a programme to attempt by NMR to identify and assign the amino acids in and near to the combining site of the Fv fragment of MOPC 315 and also to obtain their relative three-dimensional geometries. In the experiments reported in this paper 2,4-dinitrophenyl-nitroxide spin labels are used as haptens, initially as detecting probes (using ESR) to give information of the dimensions and rigidity of the combining site. We also show how it is possible using the spin-label probes to obtain the NMR spectrum of the amino acid residues around the combining site in the Fv fragment and we discuss the assignment of some of the resonances to specific types of residues. However, the fact that a particular nuclear resonance is perturbed by the spin label (and consequently "appears" in the paramagnetic difference spectrum) can only place the nucleus on a sphere of given radius from the spin-label grouping. The actual orientation of a nucleus will have to be obtained from measurements of the chemical shifts of nuclear resonances induced by paramagnetic ions such as the lanthanides [8]. The metal binding studies reported here show that there is an intrinsic binding site for Gd^{3+} and therefore presumably all the other lanthanides.

MATERIALS AND METHODS

Preparation of IgA from MOPC 315 Tumor-Bearing Mice

IgA was prepared as described by Inbar *et al.* [9]. Serum from tumor-bearing mice was subjected to ammonium sulphate precipitation, the resuspended protein was dialysed against 0.2 M Tris/HCl pH 8 and partially reduced and alkylated before being passed down a 2,4-dinitrophenyl-lysyl Sepharose immunoabsorbent column. The eluted serum proteins were discarded, and the IgA having affinity for the 2,4-dinitrophenyl group was desorbed with a solution of 0.05 M 2,4-dinitrophenyl-glycine. After removal of the hapten on a Dowex (1-X8; 200–400 mesh) column, the pure IgA was concentrated to 10 mg/ml.

Preparation of Fab' Fragment from Protein MOPC 315

The Fab' fragment of protein MOPC 315 was prepared by peptic digestion of IgA. The digestion was carried out at pH 4.7 with a protein/enzyme ratio of 100:1. The digestion was complete after 7 h at 37 °C. Isolation of the Fab' fragment was achieved by gel filtration on Sephadex G100. The Fab' peak from the column was concentrated to 10 mg/ml and for the NMR experiments, dialysed against distilled water and then $^2\text{H}_2\text{O}$, and lyophilised.

Preparation of the Fv Fragment of Protein MOPC 315

The pure Fab' fragment was digested further to the Fv fragment by peptic digestion at pH 3.7 as described by Hochman *et al.* [10]. The temperature and enzyme/protein ratio were the same as for the Fab' fragment digestion. The Fab' fragment was completely converted to Fv fragment in 4 h and the digestion stopped by raising the pH to 7.0. After the second peptic digestion, the protein solution was again fractionated on the 2,4-dinitrophenyl-lysine immunoabsorbent column and the protein having affinity for the 2,4-dinitrophenyl group was desorbed with a solution of 2,4-dinitrophenyl-glycine 0.05 M and the hapten removed on a Dowex 1-X8 column. After concentration, the Fv fragment was purified on a Sephadex G75 column to remove aggregated material and any remaining Fab' fragment. Fv fragment was eluted at about twice the void volume. For NMR studies the protein was concentrated to 10 mg/ml on a "diaflo" UM/2 membrane, and exhaustively dialysed against distilled water at 2 °C, followed by dialysis against $^2\text{H}_2\text{O}$ at room temperature for 24 h and then lyophilisation. For the ESR studies Fv

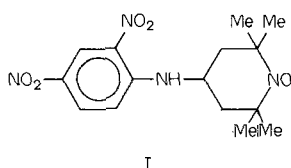
fragment was used either after the initial dialysis against distilled water, or by dissolving the lyophilized material in H_2O or $^2\text{H}_2\text{O}$.

Preparation of Non-Immune Fab Fragment from Rabbit IgG

Non-immune Fab was obtained by papain digestion of IgG as described by Porter [11].

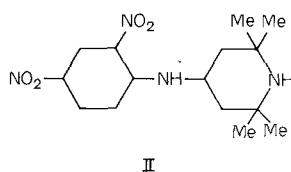
Synthesis of Haptens

(I) *N*-(1-Oxyl-2,2,6,6-tetramethyl-4-piperidinyl)-2,4-dinitrobenzene. This was prepared according to the method of Hsia and Piette [12].



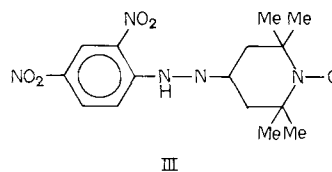
Equimolar quantities of 2,4-dinitrofluorobenzene and 4-amino-2,2,6,6-tetramethyl-piperid-1-yloxy were reacted in chloroform for 24 h at room temperature. After filtration the CHCl_3 phase was chromatographed on a silicic acid column using CHCl_3 as eluent. The fractions containing the fast-moving yellow band were taken and evaporated to dryness. The product was recrystallised from heptane- CHCl_3 (1:1, v/v).

(II) *N*-(2,2,6,6-Tetramethyl-4-piperidinyl)-2,4-dinitrobenzene. This was prepared using the method of Fraenkel-Conrat *et al.* [13].



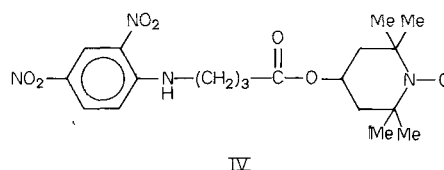
Equimolar quantities of 2,4-dinitrofluorobenzene and 4-amino-2,2,6,6-tetramethylpiperidine were reacted in 5% sodium carbonate solution at 40°C for 1 h. The yellow precipitate was filtered, washed and dried. It possessed the absorption band at 360 nm typical of ε -NH-dinitrophenyl derivatives ($\epsilon_{360} = 16 \times 10^6 \text{ cm}^{-1} \text{ M}^{-1}$).

(III) *The 2,4-Dinitrophenyl-hydrazone of 1-Oxyl-2,2,6,6-tetramethyl-4-piperidone*. The oxidation of 2,2,6,6-tetramethyl-4-piperidone was performed by a method analogous to that of Winer [14].

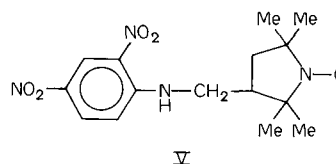


1.75 g of the hydrochloride were dissolved in 10 ml H_2O and the pH adjusted to 11 with NaOH. 0.2 g EDTA, 0.2 g sodium tungstate and 3 ml 30% H_2O_2 were then added, and the solution was left at room temperature for 7 days. After extraction with CHCl_3 and evaporation of solvent, the free radical crystallised spontaneously. The reaction with 2,4-dinitrophenyl-hydrazine was carried out as described by Stryer and Griffith [5] and the product was recrystallised from ethanol-ethyl acetate (1:1, v/v).

(IV) γ -*N*-2,3-Dinitrophenyl-(1-oxyl-2,2,6,6-tetramethyl-4-piperidinyl)-butyrate was prepared according to the method of Hsia and Piette [12].



(V) *N*-(1-Oxyl-2,2,5,5-tetramethyl-3-methyl-amino pyrrolidinyl)-2,4-dinitrobenzene was also prepared as described by Hsia and Piette [12].



Solutions of Haptens

The solubility in water of all the haptens I to V is very small. In general standard 50 mM solutions of the appropriate haptens were made up in $\text{C}^2\text{H}_3\text{COC}^2\text{H}_3$. For the NMR work aliquots of these solutions were added to the Fv fragment so as to give equimolar concentrations of hapten to the Fv fragment. For the fluorescence and ESR studies, the stock (50 mM) solutions were diluted with ethanol-water (1:1, v/v) to give solutions of $\approx 300 \mu\text{M}$ in hapten. The concentrations of the diluted stock solutions were checked spectrophotometrically.

In the ESR studies, in some cases, the ESR spectrum indicated the presence of unbound hapten. The majority of this could be removed by dialysis.

Solutions of Metal Ions

Solutions of Gd^{3+} or Tb^{3+} were prepared by roasting Gd_2O_3 or Tb_2O_3 (99.9% pure Koch-Light Laboratories) in air at 600 °C overnight and dissolving it in 10% HCl to make a stock 10 mM solution of $GdCl_3$ ($TbCl_3$). For the actual experiments some of the stock solution was diluted with distilled water and the pH adjusted to pH 5.5 by addition of NaOH.

To minimise the effect of Gd^{3+} binding to glassware [16] all NMR tubes were siliconized before use and where possible plastic pipettes were used.

Electron Spin Resonance (ESR)

ESR spectra were recorded on a JEOLCO JES-PE-1X spectrometer, operating at 9.5 GHz at room temperature (20 °C). The samples were contained in a specially constructed flat aqueous sample cell. The total volume required for each experiment was 0.1 ml. The concentration of protein was 10 mg/ml for Fv fragment and 25 mg/ml for non-immune Fab fragment.

Nuclear Magnetic Resonance (NMR)

High Resolution Studies. High resolution NMR spectra were recorded at 270 MHz using a Bruker spectrometer with an Oxford Instrument Co. superconducting magnet. The spectrometer operates in the Fourier transform mode and uses the deuterium in the samples as an internal field-frequency lock. Free induction decays were accumulated in 4000 data points with an interpoint time of 125 μ s. Delays of up to 2 s were introduced between successive pulses to minimise phase and intensity errors. Fourier transformation was then performed over 8000 points using a Nicolet 1085 computer. Difference spectra were obtained with the aid of programmes which allow spectra to be scaled and shifted before subtraction takes place. All measurements were made at 30 ± 1 °C. Chemical shift values are reported as parts per million (ppm) downfield from the sodium salt of 3-(trimethylsilyl)-propane sulphonic acid, used as an external standard.

Samples of Fv fragment were prepared for high resolution NMR studies by dissolving the lyophilised antibody fragment in 2H_2O (99.8%) to give a final concentration of 1–2 mM. The pH (direct meter reading uncorrected for the 2H isotope effect on the glass electrode) of the samples was adjusted with dilute solutions of 2H_2SO_4 and NaO^2H . The ionic strength was maintained at 0.15 M using NaCl.

The Water Solvent Spin Lattice Relaxation Rates

These were measured by the null method at 20 MHz and 20 ± 1 °C using a $180^\circ\text{-}\tau\text{-}90^\circ$ pulse sequence. The spectrometer has been described elsewhere [17]. The sample volume used was 0.01 to 0.05 ml. The relative values of the relaxation rates were accurate to within a standard deviation of 2%.

SPECTRAL INTERPRETATION

Spin Label ESR

The spin-labelled hapten has a three-line ESR signal arising from the hyperfine interaction of the spin label unpaired electron with the nitroxide nitrogen nucleus. The anisotropy of this hyperfine splitting with respect to the magnetic field direction causes the ESR spectrum to be sensitive to both the amplitude and rate of motion of the spin-labelled group [18]. Since the amplitude of motion of the bound hapten is limited by the steric effects of neighbouring groups in the antibody combining site and the rate of motion is partially governed by the flexibility of these groups, the spin label spectrum is capable of giving information about both the dimensions and rigidity of the combining site.

For the extreme case of a spin label rigidly fixed in a single crystal, different hyperfine splittings would be measured when the magnetic field was directed along each of the three principal molecular axes of the nitroxide group, and intermediate splittings would be obtained for intermediate orientations. The splittings between the two outer lines of the three-line hyperfine structure are found to be in the region of: $2A_{zz} = 64$ gauss, $2A_{xx} = 2A_{yy} = 12$ gauss (where A is the principal value of the hyperfine splitting constant) [19,20], the absolute values depending to some extent on the polarity of the crystalline environment. At the opposite extreme, if the spin label is in a low viscosity solvent it will tumble rapidly and randomly giving rise to an isotropic spectrum in which the differences in splittings are completely averaged and the overall splitting between the two outer lines is given by the mean: $2A_0 = 1/3 (2A_{zz} + 2A_{xx} + 2A_{yy})$ where A_0 is the isotropic splitting constant and depends slightly on the polarity of the solvent [23].

Intermediate cases of partial averaging of the anisotropy of the hyperfine splittings occur when the spin label group performs an anisotropic motion, as is the case for a bound hapten in which any molecular motion is limited by the geometry of the combining site. In this case overall splittings $2A_{z'z'}$, $2A_{x'x'}$, $2A_{y'y'}$ would be obtained which have a smaller difference (anisotropy) between them than the single

crystal values, and whose value is directly related to the amplitude of the motion and hence to the dimensions of the combining site. Here x' , y' , z' are no longer the molecular axes of the nitroxide group but are the axes about which the motional averaging takes place.

The motional averaging process also depends on the rate of motion as well as the amplitude of motion. For instance, although the whole Fv fragment is randomly tumbling in solution it can be calculated from its molecular weight (25000) that the tumbling rate is $\approx 0.1 \text{ ns}^{-1}$ which is too slow to produce much significant motional averaging. Thus any motional averaging observed in the spectrum of the bound hapten arises from the intramolecular motion of the hapten itself, as restricted by the geometry of the combining site.

A complication arises since we are dealing with randomly orientated antibody fragments rather than a single crystal. In this case spectra from all intermediate orientations, as well as the principal splittings $2A_{z'z'}$, $2A_{x'x'}$, $2A_{y'y'}$, are superimposed and this gives rise to a rather complicated spectrum. However, the maximum splitting, $2A_{z'z'}$, can always be resolved (see Fig. 3, 4) and in favourable circumstances the minimum splitting can sometimes be resolved. This latter case usually obtains when the motional averaging is axial: $2A_{x'x'} = 2A_{y'y'}$, and these two sets of splittings are superimposed (see Fig. 3, label III).

NMR Difference Spectroscopy

This technique involves the subtraction of the NMR spectrum of our sample from that of another measured under identical instrumental conditions. This is particularly useful in NMR for it often makes possible the observation of resonance peaks otherwise obscured by the envelope of the protein spectrum and also assists in the measurement of their linewidths. In this paper we shall be concerned with three types of NMR difference spectra. These arise either from changes in chemical shifts of resonances (pH and hapten-binding difference spectra) or changes in linewidth of resonances caused by the proximity of a paramagnetic centre (paramagnetic difference spectrum).

pH difference spectrum is obtained by subtraction of NMR spectra of the sample measured at two different pH values (e.g. Fig. 5).

Hapten-binding difference spectrum is obtained by subtraction of the NMR spectrum of the antibody fragment from that of a sample of identical concentration of antibody, but in the presence of a hapten (e.g. Fig. 6). A particular case of this occurs when the hapten is paramagnetic as discussed below.

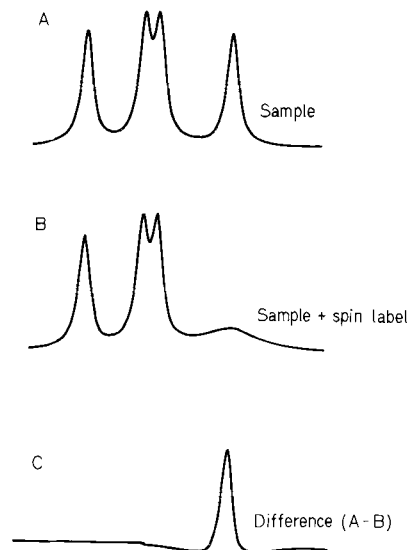


Fig. 1. A simulated paramagnetic difference spectrum

Paramagnetic Difference Spectrum

Many paramagnetic centres can perturb an NMR spectrum by causing shifts of the resonance positions of the nuclei and by causing broadening of the linewidths. The paramagnetic species can be chosen so that one of these perturbations will dominate. Spin labels, such as those described in this paper generally broaden NMR linewidths. This broadening is inversely proportional to the sixth power of the distance between the paramagnetic centre and the particular nucleus (whose resonance is being observed). Thus the most profound effect is on the nuclei close to the paramagnetic centre. Let us consider an NMR spectrum of four resonances arising from four chemically distinct nuclei, as shown in Fig. 1. Suppose we now add a paramagnetic spin label, which binds very close to one nucleus. The NMR line width of this nucleus is then broadened. (For simplicity we assume the other nuclei are too far away from the spin label to be significantly affected.) If we subtract the two spectra as shown in Fig. 1 we obtain essentially only the unperturbed spectrum of the resonances of nuclei close to the paramagnetic centre. This technique is thus a method which can lead to a great deal of simplification of an NMR spectrum and give information on the nuclei which are near to and therefore perturbed by, the paramagnetic centre. We can make this more quantitative as shown below. For a Lorentzian line the maximum peak intensity is inversely proportional to the linewidth

$$I_0 \propto \frac{1}{\Delta \nu_0} \quad (1)$$

The presence of the spin-labelled hapten will add a contribution Δv_p to the linewidth of a resonance, making a new linewidth ($\Delta v_p + \Delta v_0$). If we assume that the line shape is still Lorentzian then the new intensity I' is given by

$$I' \propto \frac{1}{\Delta v_0 + \Delta v_p}. \quad (2)$$

If we subtract the two Lorentzian lines we obtain

$$I = I_0 - I' \propto \frac{1}{\Delta v_0} - \frac{1}{(\Delta v_0 + \Delta v_p)}$$

whence

$$I/I_0 = \frac{\Delta v_p}{\Delta v_0 + \Delta v_p}. \quad (3)$$

We note from Eqn (3) that when $\Delta v_p \ll \Delta v_0$, $I/I_0 \rightarrow 0$ and thus a resonance will not appear in the difference spectrum. Conversely, when $\Delta v_p \gg \Delta v_0$, $I/I_0 \rightarrow 1$, and the full intensity of the resonances perturbed by the spin label appears. The value of Δv_p for a given nucleus depends on the distance (r) between the nucleus and the spin label. It can be calculated by using the Solomon-Bloembergen equation for dipolar broadening [9] viz.

$$\Delta v_p = \frac{1}{15} \frac{\gamma_I^2 g^2 S(S+1) \beta^2}{r^6} f_2(\tau_c) \quad (4)$$

$$f_2(\tau_c) = 4\tau_c + \frac{3\tau_c}{1 + \omega_I^2 \tau_c^2} + \frac{13\tau_c}{1 + \omega_S^2 \tau_c^2} \quad (5)$$

where γ_I is the magnetogyric ratio, β is the Bohr magneton, S is the total electron spin, g is the g value of the electron and τ_c is the correlation time which characterises the modulation of the dipole-dipole interaction. Using values of $\gamma_I = 2.6735 \times 10^4 \text{ rad} \cdot \text{S}^{-1} \cdot \text{G}^{-1}$; $\beta = 0.92731 \times 10^{-40} \text{ erg} \cdot \text{G}^{-1}$, $g = 2$ and $S = 1/2$, Eqn (4) becomes:

$$\Delta v_p = \frac{0.391}{r^6} \cdot 10^{16} f_2(\tau_c) \quad (6)$$

where r is in \AA . If we assume that τ_c is the rotational tumbling time of the molecule τ_R , then using Stokes law [8] this may be estimated from the expression

$$\tau_R = \frac{M\bar{V}\eta}{RT} \quad (7)$$

where M is the molecular weight of the spin label-antibody complex (~ 25000), \bar{V} is the partial specific volume ($= 0.72 \text{ cm}^3/\text{g}$), η is the viscosity of the solvent

Table 1. Variation of dipolar linewidth of a nucleus at 270 MHz, caused by the spin label as a function of the distance between them. The calculation assumes a correlation time of 7 ns

r	Δv_p
\AA	Hz
4	27600
6	2425
8	432
10	113
12	38
14	15
16	6.5
18	3.2

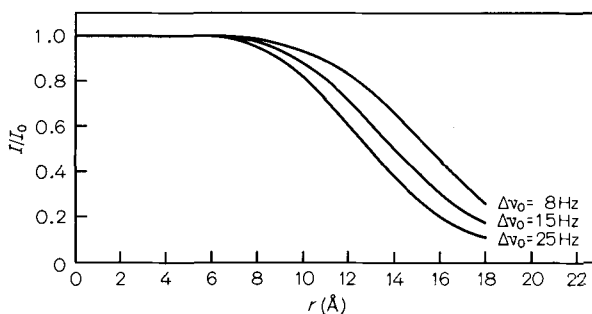


Fig. 2. Calculated intensity ratio of the difference of two isolated Lorentzian nuclear resonance lines as a function of distance (r) between a nucleus and a spin label centre. The calculation uses Eqn (1) and is illustrated for three different values of Δv_0 , the natural linewidth

(0.008 poise at 30 °C), T is the absolute temperature and $R = 8.315 \times 10^7 \text{ erg} \cdot \text{deg}^{-1} \cdot \text{mol}^{-1}$. This gives the $\tau_R = 7 \times 10^{-9} \text{ s}$ and thus

$$\Delta v_p = \frac{11.33 \times 10^7}{r^6} \text{ Hz}. \quad (8)$$

This calculation assumes that the spin label moiety is rigidly held. If this is not the case the dipolar interactions (and hence Δv_p) will be reduced. Table 1 lists the value of Δv_p as a function of r . Using these values of Δv_p we obtain curves like those shown in Fig. 2, for the intensity of a resonance peak in the paramagnetic difference spectrum. As we have noted the observed effect also depends on the relative magnitudes of Δv_0 and Δv_p . Three typical values are used in Fig. 2. A value of 25 Hz is fairly typical for a methyl group in a protein of molecular weight 25000, while a value of $\Delta v_0 = 8 \text{ Hz}$ is often found for the C-2 proton resonances of histidine residues [22]. From the figure it is clear that up to $\approx 8 \text{ \AA}$ the intensity ratio remains at unity but after this the intensity ratio falls off. The effective perturbing range of the spin label will depend

on both the natural linewidth and the signal to noise ratio in the spectrum. Thus, for example, a linewidth of 25 Hz and a signal to noise ratio of 5:1, only protons nearer than 16 Å to the spin label will effectively contribute to the difference spectrum. For a natural linewidth of 8 Hz there may still be a significant contribution at 16 Å. However the intensity ratio I/I_0 only considers the ratio of peak heights. When this ratio differs significantly from unity the lineshape may be considerably distorted [23] and not observable.

Water Proton Relaxation Studies in Solutions containing Paramagnetic Ions

The introduction of a macromolecule to which the metal ion can bind can lead to an increase in the water proton relaxation rate [8]. The paramagnetic contribution $1/T_{1P}$ to the water proton spin lattice relaxation rate of a metal ion solution containing an arbitrary amount of protein may be written as:

$$\frac{1}{T_{1P}} = \frac{(1 - X_b)}{T_{1F}} + \frac{X_b}{T_{1B}} \quad (9)$$

where $1/T_{1F}$ is the relaxation rate of the water protons in a solution containing only the metal ions and $1/T_{1B}$ is the relaxation rate of water protons in a solution containing an equivalent concentration of metal ion bound to the protein. X_b is the fraction of metal ion which is bound to the protein, and is an explicit function of the binding constant K_D , and the number of equivalent binding sites, n [8]. Eqn (9) may be rewritten as

$$1/T_{1P} = 1/T_{1F} + X_b \left(\frac{1}{T_{1B}} - \frac{1}{T_{1F}} \right). \quad (10)$$

It is clear from Eqn (10) that titrations using the water relaxation rate may be used to characterize the binding of paramagnetic metal ions to proteins, with respect to the binding constant and the number of metal binding sites, n , in exactly the same way that any of the more standard physical parameters *i.e.* fluorescence, optical absorption *etc.* are utilized.

RESULTS

Spin Label ESR Studies

The geometry and flexibility of the antibody combining site have been probed using spin-labelled haptens of different lengths and lateral dimensions. The ESR spectra of the various spin-labelled haptens bound to the Fv fragment of protein MOPC 315 are given in Fig. 3 and 4.

Broadened spectra are obtained indicative of immobilized spin labels, with the spectra of a small amount of free spin label superimposed in all cases (compare Free spin label spectrum in Fig. 3). However, for the hapten label IV the motion of the bound hapten nitroxide group approaches isotropic, and bound and free spectra are not well-resolved. The contribution from the bound hapten to the high field line is dotted in schematically in Fig. 3.

In the case of the hapten label I, lines appear in the spectrum at the position of the free hapten label, but the lines are rather broad. This broadening is not a viscosity effect attributed to the high protein concentration in this sample since dilution experiments do not lead to a narrowing of the lines, and also much narrower lines are obtained from the free spin label in solutions of non-immune Fab fragment (from rabbit IgG) at equivalent or higher concentrations. These lines must be attributed to either a rather complicated motion of the bound spin label, or non-specific binding to other weaker sites, the population of which would be approximately 10% of the specific binding site.

Evidence for possible non-specific binding has been obtained in experiments with spin label hapten I and non-immune Fab fragment from rabbit IgG. In the presence of non-immune Fab fragment the ratio of the amplitude of the low field peak to the centre peak in the ESR spectrum of the free spin label is decreased by 5–10% over a range of concentrations of hapten : Fab fragment of 1:5 up to 3:1. This is attributed to the effect of the underlying spectrum of ≈ 5 –10% non-specifically bound spin label which is barely detected in the presence of the free spin label.

The bound ESR spectra of Fig. 3 and 4 all show a well-defined outer splitting which may be used to analyse the anisotropic motion of the bound spin-labelled hapten. The six-membered ring spin label I has the smallest separation (2.7 Å) between the dinitrophenyl ring and the nitroxide ring. This gives rise to a spectrum with outer splitting of $2A_{z'z'} = 52.1 \pm 0.3$ gauss. This indicates that the spin label is strongly held in the combining site, but has a limited amount of internal motion which reduces the maximum splitting from 64 gauss. On the other hand the five-membered ring spin label V, has a slightly larger separation (4.1 Å) between the dinitrophenyl ring and the nitroxide ring, but gives an outer splitting of $2A_{z'z'} = 63 \pm 3$ gauss characteristic of almost total immobilisation. We conclude that the smaller outer splitting in the case of the six-membered ring is caused by a limited molecular motion arising from the conformational flexibility of the six-membered piperidine ring in contrast to the rigidly held five-membered pyrrolidine ring. This makes it possible to put some

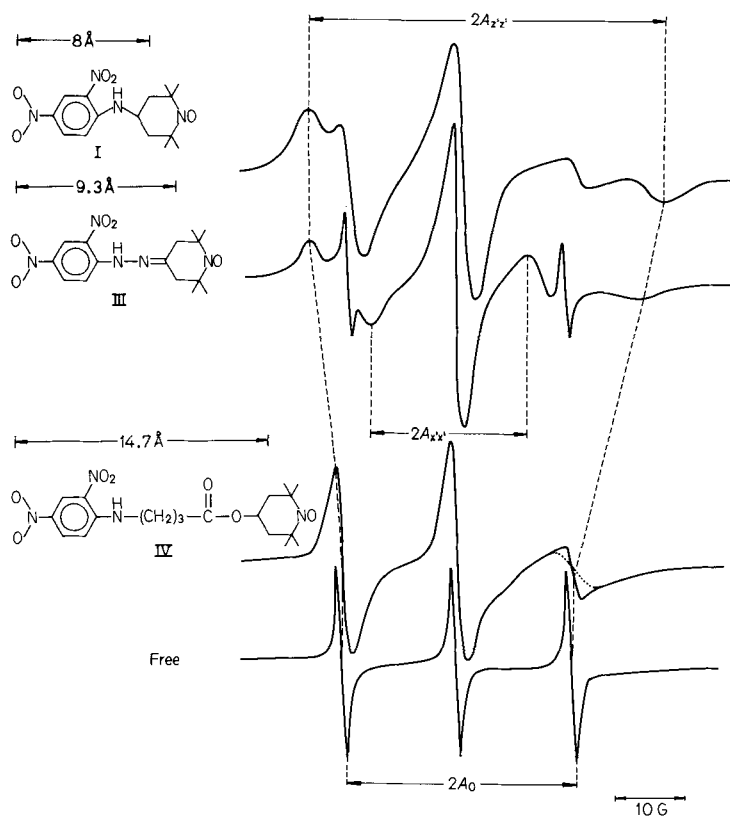


Fig. 3. ESR spectra of the six-membered-ring hapten spin labels bound to the Fv fragment of protein MOPC 315. The bottom spectrum (Free) is the isotropic spectrum characteristic of all the hapten

spin labels when tumbling freely in aqueous solution. The protein concentration was 10 mg/ml, the solution contained 0.15 M NaCl pH = 7 and $T = 19^\circ\text{C}$. The modulation amplitude was 2 gauss

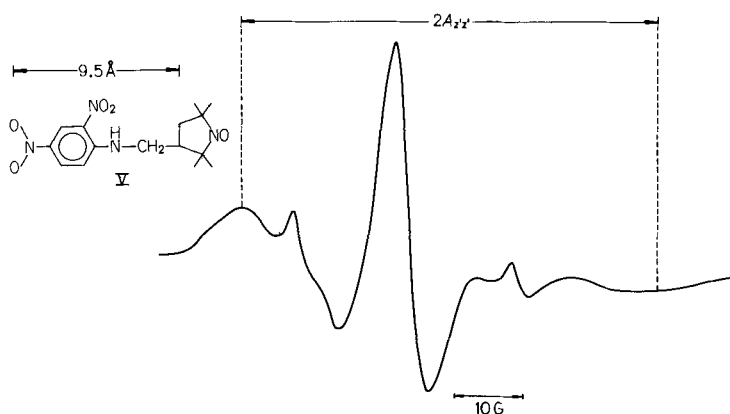


Fig. 4. ESR spectrum of the five-membered-ring hapten spin label bound to the Fv fragment of protein MOPC 315. Other conditions as in Fig. 3

limits on the lateral dimensions of the combining site, since it must be sufficiently large to accommodate both the five-membered ring, and also the conformers of the six-membered ring which have a rather different geometry. These lateral dimensions are determined primarily by the methyl groups attached to the spin label rings, and the most likely conformers of the six-

membered ring are the two "twisted" conformations which give rise to the least intramolecular steric hindrance between the methyl groups. On this basis, the limits put on the lateral dimensions are: $9 \text{ \AA} \times 6 \text{ \AA}$.

The ESR spectra of the two spin label haptens I and V thus give strong evidence that the antibody dinitrophenyl combining site is a rather rigid structure.

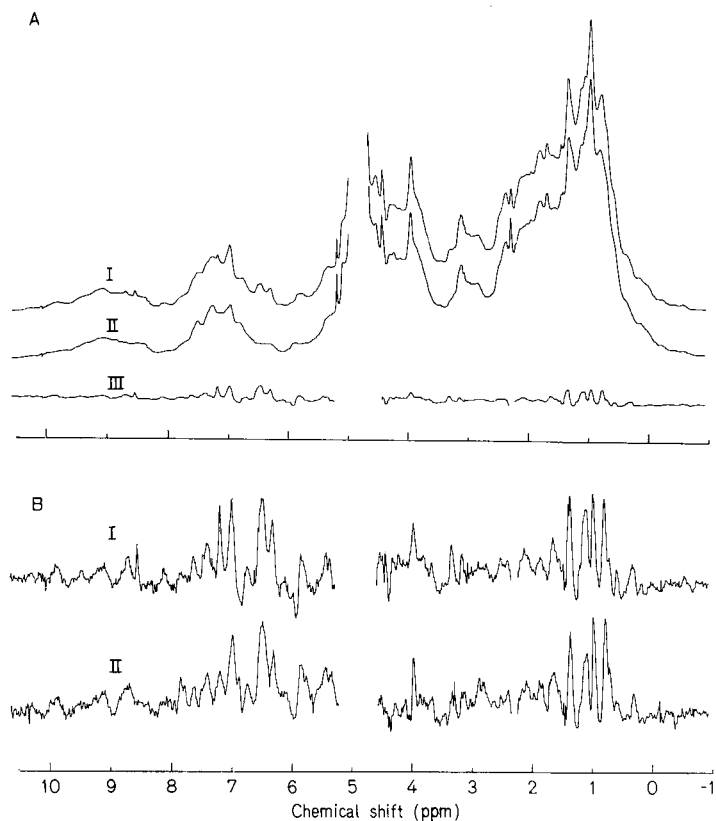


Fig. 5. 270 MHz proton spectrum of Fv fragment from protein MOPC 315. (A) 30 mg/ml, $T = 30^\circ\text{C}$, $\text{pH} = 6.29$ [NaCl] = 0.15 M, 2000 scans. (I) No addition; (II) in the presence of an equivalent

amount of spin label I; (III) paramagnetic difference spectrum, (I–II). (B) Enlarged ($\times 6$) paramagnetic difference spectra at (I) $\text{pH} = 6.29$, (II) $\text{pH} = 8.47$. Other conditions as for A

Since the ESR spectrum of the five-membered ring spin label V, closely approaches that of a rigidly immobilised spin label this implies that there is little or no rotation about the three flexible bonds in the five-membered ring hapten. By analogy it is assumed that there is also little rotation about the two bonds joining the six-membered ring to the 2,4-dinitrophenyl ring in spin label I. Thus the dinitrophenyl ring is held in a rigid combining site.

In Fig. 3 are seen the ESR spectra from haptens with varying distance between the dinitrophenyl ring and the nitroxide six-membered ring. Label I is rigidly held as discussed above. Label III, of intermediate length, has a spectrum characteristic of an anisotropic motion of limited amplitude. It has an outer splitting of $2A_{z'z'} = 47.6 \pm 0.2$ gauss, and a well-defined inner splitting of $2A_{x'x'} (\approx 2A_{y'y'}) = 22.6 \pm 0.1$ gauss. This corresponds to an amplitude of motion in the region of 50° (see *e.g.* [18,24]) suggesting that this could correspond to rotation about one of the single bonds in the dinitrophenyl-nitroxide linkage. A motion of this type would be possible about the bond adjacent to the nitroxide ring, if a substantial part of the latter were protruding beyond the end of the combining site

(particularly if the methyl groups were unobstructed). Such an interpretation is supported by the magnitude of the isotropic splitting factor $A_0 = 15.7$ gauss to be compared with that of the free spin label: $A_0 = 16.0$ gauss, suggesting that the nitroxide group of the bound label is protruding into the aqueous phase. These considerations would lead to an estimate for the length of the combining site of $\approx 11 \text{ \AA}$. The spectrum of the longest member of the series, IV, is seen to approach that of a three line spectrum with almost complete motional averaging, with a single splitting of 16.0 gauss which corresponds to that of the free spin label (which is also superimposed on this spectrum). However, the spectrum from the bound label differs from that of the free label in that there is considerable differential broadening of the lines. This indicates that although the amplitude of motion is very large, the motion is still somewhat restricted in that it takes place relatively slowly, with a correlation time in the region of 1 ns. A possible explanation of this almost complete motional averaging is that the nitroxide ring projects sufficiently far out from the combining site that conformational transitions are possible within the ring which causes

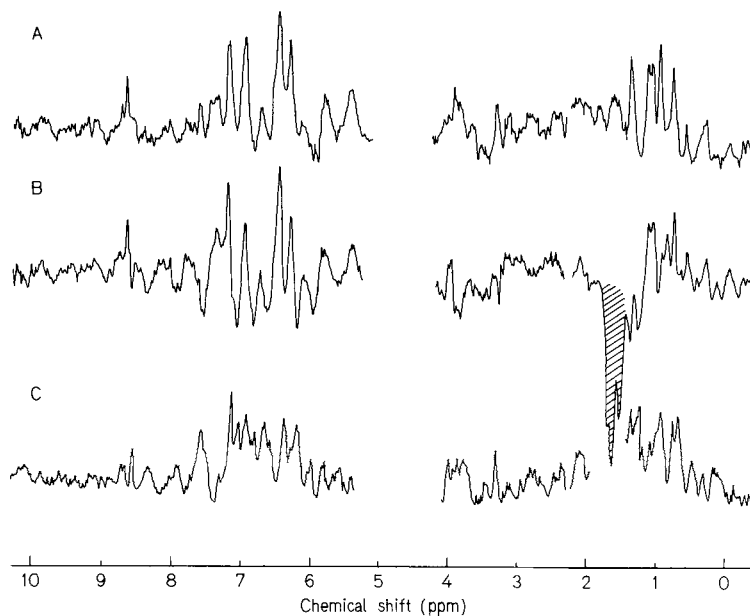


Fig. 6. 270 MHz proton difference spectra of Fv fragment from protein MOPC 315. (A) Paramagnetic difference spectrum using spin label I; (B) hapten difference spectrum using the diamagnetic analogue of hapten I, *i.e.* II. The shaded methyl resonances originate

from the hapten. (C) B–A, the shaded resonances are omitted in this case pH = 5.80 for A, B and C. Other conditions analogous to those for Fig. 5

the nitroxide group to double back on itself. The motional broadening suggests that this particular hapten is of such a length that the nitroxide group is only just sufficiently clear of the combining site for this to be possible. Such considerations would again be consistent with the length of the combining site being $\approx 11 \text{ \AA}$.

PROTON MAGNETIC RESONANCE STUDIES

Difference Spectra

The 270 MHz NMR spectra of the Fv fragment of protein MOPC 315 in the presence and absence of the hapten dinitrophenyl-nitroxide (I) are shown in Fig. 5A. The same figure also shows the NMR paramagnetic difference spectrum caused by the presence of the spin labelled hapten. Only a small amount (10%) of the total NMR spectrum of the Fv fragment is affected by the presence of the spin label. Fig. 5B shows the paramagnetic difference in more detail at two pH values. We note that there is the equivalent of approximately equal numbers of aromatic (6–9 ppm) and aliphatic (0–5 ppm) protons and also that there are slight variations in the difference spectra with pH. However in both cases it appears that the difference spectrum contains a few resonance peaks that appear only as a result of changes in the chemical

shift of some of the Fv fragment resonances. Clearly any such differences arising from changes in chemical shift must come from resonances outside the perturbing (broadening) range of the spin-labelled hapten.

That indeed the presence of hapten does result in chemical shift changes is well illustrated by the (diamagnetic) hapten difference spectrum, hapten II, shown in Fig. 6B. The large negative peaks in the methyl region ($\approx 1.5 \text{ ppm}$) arise from the methyl peaks of the hapten, which in contrast to those observed in the free hapten, are no longer equivalent. Comparison of Fig. 6A and B however shows that the majority of the resonances which occur in the (diamagnetic) hapten difference spectrum, as a result of chemical shift changes, are also broadened by the spin label. By using the diamagnetic hapten as the control, the resulting paramagnetic spectrum in Fig. 6C should only contain those resonances perturbed by and therefore near to, the spin label moiety. Unfortunately however, the spectrum may be slightly complicated by the presence of the resonances from the diamagnetic hapten—which may obscure some of the Fv fragment resonances. This is particularly noticeable in the methyl region, and in Fig. 6C the shaded methyl resonances have been omitted for clarity. The methyl resonances of the spin label hapten itself are, of course, broadened out by the paramagnetic centre and thus do not appear in the difference spectrum.

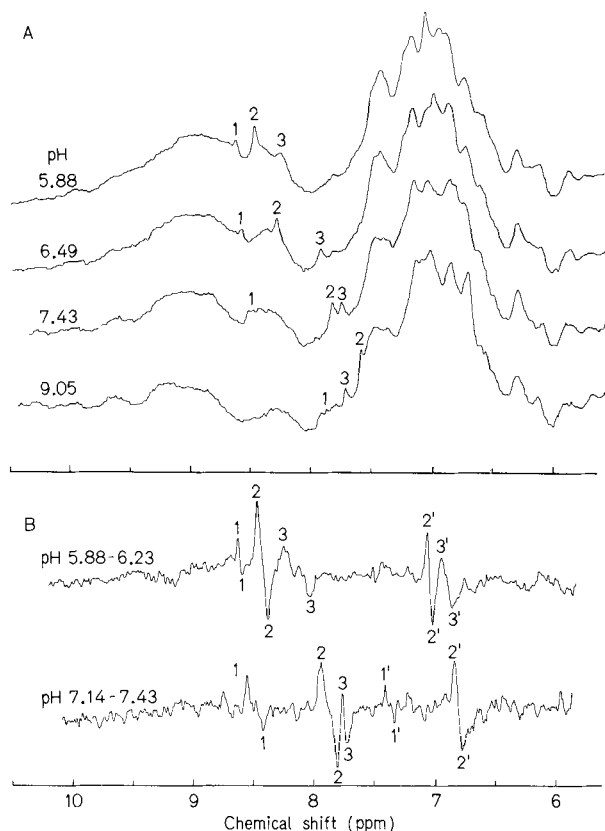


Fig. 7. Effect of changing pH on the aromatic resonances of the Fv fragment. (A) 270 MHz proton spectrum of the aromatic region of fragment Fv from MOPC 315, in the presence of hapten II at three different pH values. The numbers indicate the C-2 protons of three titrating histidines. Other conditions as for Fig. 5. (B) Illustration of pH difference spectroscopy showing both C-2 and C-4 protons of titrating histidine residues

Effect of pH

The result of changing the pH on the aromatic resonances of the Fv fragment in the presence of the diamagnetic hapten (II) are shown in Fig. 7A. The changes are most easily followed by the use of difference spectroscopy involving the subtraction of spectra at different pH values (Fig. 7B). Only those resonances which alter their position with pH will appear in a difference spectrum. The results can be presented in the form of a pH titration, in which the chemical shifts are plotted against the pH of the solution. Fig. 8 shows the results of such a titration. The resonances 1, 2 and 3 are assigned to the C-2 protons of histidine rings since the resonance positions occur in the range characteristic of C-2 protons [8,24] and since the chemical shifts between the protonated and unprotonated species is of the order of 1 ppm, again characteristic of the behaviour observed for histidine C-2 protons [8,24]. Similar arguments allow us to assign the

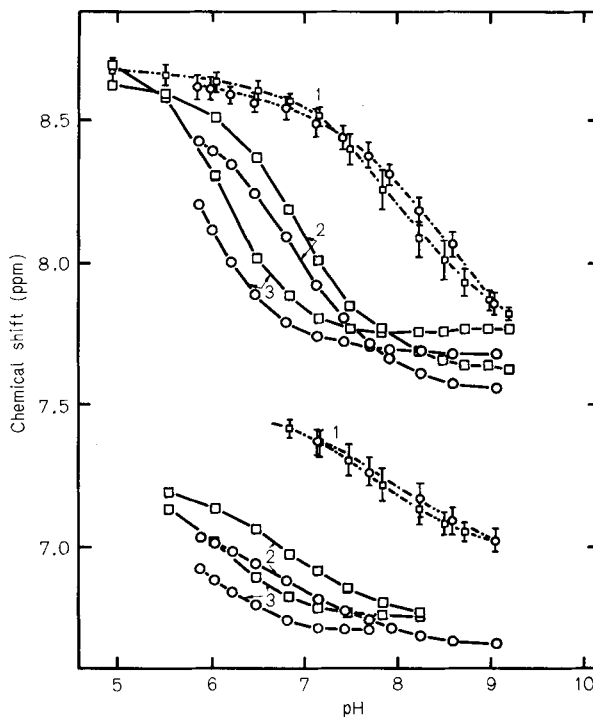


Fig. 8. Titration of the histidine chemical shifts versus pH for the Fv fragment from protein MOPC 315 in the absence (□) and in the presence of hapten II (○).

resonances 1', 2' and 3' to C-4 histidine protons. The dashed numbering is assigned on the basis of the pK_a values which are about 8.1 (resonances 1 and 1'), 6.9 (resonances 2 and 2') and 6.1 (resonances 3 and 3'). The pK_a values in the table are obtained from fitting the titration curves to the Henderson-Hasselbalch equation, assuming a chemical shift of 1 ppm for the histidine C-2 proton in cases where the full titration curves are not observed.

Resonances 1 and 1' are anomalous in that they each split into at least two components over the titration range. For this reason the titration curve shown represents the average of the positions of the various components. It is however observed that each component of the resonances 1 and 1' has approximately the same pK_a value and further, that the total area of all the components of each resonance corresponds to one proton within the limits of experimental error (*i.e.* the area of either resonance 2 and 3).

The same behaviour is observed for a titration of chemical shift, against pH with Fv fragment itself in the absence of hapten (Fig. 8). However, although the values of chemical shifts of the resonances are slightly different in the two cases particularly for the histidines 2 and 3 (Table 2), within the error, there seems little change in the pK_a values.

Table 2. Proton chemical shifts and pK_a values of histidine residues for the Fv fragment from protein MOPC 315 in the presence and absence of the hapten N-(2,2,6,6-tetramethyl-4-piperidinyl)-2,4 dinitrobenzene (hapten II)

Chemical shifts (measured at 270 MHz) are downfield from the sodium salt of 3-(trimethyl silyl)-propane sulphonic acid, and refer to the shift of the protonated species. pK_a values were calculated from fitting the curves shown in Fig. 8 to the Henderson-Hasselbach equation assuming a chemical shift of 1 ppm for the C-2 proton resonances. The pK_a values are based on the uncorrected pH meter readings. Experiments were carried out in 0.15 M NaCl at $T = 30^\circ\text{C}$

Sample	Resonance								
	1		2		3				
	pK_a	shift		pK_a	shift		pK_a	shift	
		C-2(H)	C-4(H)		C-2(H)	C-4(H)		C-2(H)	C-4(H)
		Hz				Hz			
Fv fragment	8.10 ± 0.2	2068	1886	6.94 ± 0.2	2058	1816	6.10 ± 0.2	2094	1824
Fv + hapten II	8.25 ± 0.2	2076	1889	6.92 ± 0.2	2036	1798	5.90 ± 0.2	2080	1812

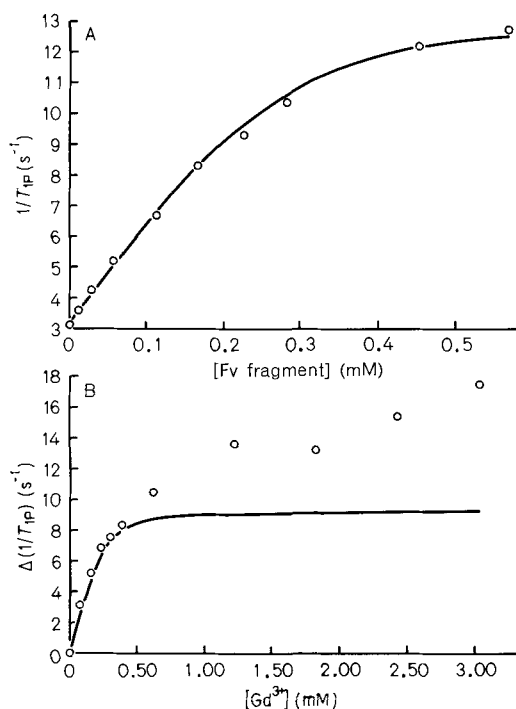


Fig. 9. The binding of Gd^{3+} to Fv fragment from protein MOPC 315 monitored by the change in proton relaxation rate of the solvent water at 20 MHz as Gd^{3+} is bound, $1/T_{1P}$. (A) Titration of Gd^{3+} with Fv fragment. Conditions were $[Gd^{3+}] = 274 \mu\text{M}$, $\text{pH} = 5.5$, $[\text{KCl}] = 0.15 \text{ M}$, $T = 19^\circ\text{C}$. The continuous curve is calculated for $n = 1$, $K_D = 30 \mu\text{M}$. (B) Titration of Fv fragment with Gd^{3+} $\frac{1}{T_{1P}} = X_b \left(\frac{1}{T_{1B}} - \frac{1}{T_{1F}} \right)$ see Eqn (10). Conditions were Fv fragment = $248 \mu\text{M}$, $\text{pH} = 5.5$, $[\text{KCl}] = 0.15 \text{ M}$, $T = 19^\circ\text{C}$. The continuous curve is calculated for $n = 1$, $K_D = 30 \mu\text{M}$ and a value of $(1/T_{1B} - 1/T_{1F})$ from the data of Fig. 9A

In the presence of the spin labelled hapten I, similar titrations involving the use of the pH difference titration method show that the resonances of histidine residues 2 and 3 can no longer be observed over the same pH range. The resonances do however appear in the spin-labelled difference spectrum, suggesting that they are broadened by the spin label. The slight differences with pH observed in Fig. 5B can now be interpreted in terms of the consequent chemical shift changes of the histidine residues.

The identification of the histidine residues also permits a reasonably accurate estimation of the number of protons in the paramagnetic difference spectra. The aromatic region corresponds to the equivalent of about 30 protons and the aliphatic region to about 21 protons.

Lanthanide Binding Studies

Water Proton Relaxation Studies in Gd^{3+} Solutions. Fig. 9A shows a titration of a fixed amount of $Gd(\text{III})$ as a function of Fv fragment concentration. The titration was followed by measuring the change in the solvent spin lattice water relaxation rate as the Gd^{3+} is bound to the protein. Fig. 9B shows the titration of a fixed amount of Fv fragment as a function of Gd^{3+} concentration. The difference between the relaxation rate of a given Gd^{3+} solution in the presence and absence of Fv fragment denoted $\Delta(1/T_{1P})$, $\equiv X_b \left(\frac{1}{T_{1B}} - \frac{1}{T_{1F}} \right)$ see Eqn (10), is plotted as a function of the Gd^{3+} concentration.

The continuous curves in Fig. 9A and B are computed from Eqn (10) using one metal binding

site with a value of $K_D = 30 \mu\text{M}$. The approximately linear increase in $\Delta(1/T_{1B})$ in Fig. 9B, apparent at Gd^{3+} concentrations $> 1 \text{ mM}$ may be ascribed to the presence of substantially weaker binding sites ($K_D > 3 \text{ mM}$).

DISCUSSION

The paramagnetic difference spectrum (Fig. 5A and B) corresponds to a small amount of the total Fv fragment spectrum suggesting that relatively few amino acid residues are affected by the presence of the bound hapten. The same spectrum also contains one or two Fv fragment resonances whose presence arises from changes in chemical shift upon hapten binding. These shifts arise from two main causes. Firstly, conformational changes involving changes in environment of amino acid residues in the Fv fragment. In particular any changes which alter the relative positions of aromatic amino acids could lead to changes in the ring currents [8] (and therefore to shifts) experienced by a given nucleus. Secondly, ring current shifts of amino acid residues in the Fv fragment resulting from the introduction of the ring current perturbation of the dinitrophenyl moiety. Ring current effects could cause significant shifts in residues up to 7 \AA from the perturbing centre [8].

In the section on paramagnetic difference spectra, we have shown that if the spin label hapten is rigidly held, as in the case here, the spin label moiety will probably broaden residues over a sphere of radius of the order of $12\text{--}16 \text{ \AA}$, (slightly longer than the estimated length of the spin label hapten (I) itself). Thus the observed shifts discussed above must come from resonances of residues outside the perturbing range of the spin label. From a comparison of the paramagnetic and diamagnetic hapten difference spectra (Fig. 6) it is clear that if there are conformational changes in the Fv fragment on hapten binding these must be mainly restricted to the region within perturbing range of the spin label and therefore in effect to the combining site—since this is estimated from ESR studies to be $\approx 11 \text{ \AA}$.

On the basis of pH titrations the resonances of two histidine residues can be shown to be present in the paramagnetic difference spectrum. From sequence studies it is known that there are three histidines in the Fv fragment [10] at positions 44 and 97 in the light chain [25] and at position 102 in the heavy chain [26]. Positions 97_L and 102_H may be presumed to be in hypervariable regions, by analogy with human Ig variable region sequences [27]. These latter two positions would also be found in the cleft, described

by Polyak *et al.* [3,4] in the three-dimensional structure of fragment Fab' New which is the potential antigen binding site [3,4]. Histidine at position 44 in the light chain is not in a hypervariable region, nor is it one of the residues found in the cleft referred to above. We would postulate, however, from our results, that resonances 1 and 1' can be assigned to histidine 44_L .

The reason for the behaviour observed for the resonances of the histidine with a pK_a value of 8.2 (resonances 1 and 1') in splitting into two or more components is not clear to us. It might reflect some local heterogeneity in the residues around this histidine residue, *e.g.* an asparagine residue in some of the Fv molecules might be an aspartate residue in some of the other Fv molecules. Alternatively it may be that this particular histidine residue undergoes some form of restricted motion, the different components then reflecting the different environments possible for the C-2 protons and similarly for the C-4 protons.

Although the aromatic region of the paramagnetic difference spectrum shows resonance patterns characteristic of tyrosine, tryptophan and phenylalanine as well as histidine, it is not possible to assign the patterns to a specific number of residues without showing that the resonances of whole residues are present in the paramagnetic (spin label) difference spectrum. For instance in the case of tryptophan the separation between protons across the two rings can be as large as $\approx 5 \text{ \AA}$. Since the broadening of a nuclear resonance by a paramagnetic centre depends on the sixth power of the distance of the nucleus from the paramagnetic centre, it is possible that only some of the aromatic protons of a tryptophan residue will appear in the difference spectrum. However from integration it can be concluded that there is only the equivalent of about 30 protons in the aromatic region of the paramagnetic difference spectrum that have to be assigned. There is a similar number of protons in the aliphatic region. The resonances observed in the range $0\text{--}3 \text{ ppm}$ are characteristic of methyl groups. Integration shows that only 21 protons have to be assigned in this region, and if we assume that there is the rapid rotation generally associated with methyl groups, this means that whole methyl groups will occur in the paramagnetic difference spectrum and thus only 7 methyl groups have to be assigned. These could arise from any of the residues that contain free methyl groups, *viz.* alanine (1), valine (2), isoleucine (2), leucine (2) and threonine (1), the numbers in parentheses indicating the number of methyl groups associated with each residue.

The spin label ESR provides information about the overall geometry and structural rigidity of the site. As shown above, the steric immobilization of the

spin-labelled haptens suggests that the combining site is a cleft of overall dimensions $11 \text{ \AA} \times 9 \text{ \AA} \times 6 \text{ \AA}$ which has considerable structural rigidity. These dimensions for the antibody cleft can be compared with the transverse dimensions of the dinitrophenyl ring of 7.3 \AA , and the overall length of dinitrophenyl-lysine and dinitrophenyl-glycine of 16 \AA and 10.5 \AA respectively. This means dinitrophenyl-glycine can be completely accommodated within the combining site from the dimensions given here, whereas the dinitrophenyl-lysine molecule might protrude from the end of the cleft.

Haselkorn *et al.* [28] have used kinetic mapping to investigate the dimensions and subsites of interaction of the dinitrophenyl binding site of IgA protein-315. They conclude, on the basis of rates of binding and dissociation, that the minimal dimensions of the binding site are $12 \text{ \AA} \times 6 \text{ \AA}$ which is in reasonable agreement with the present findings.

Previous spin label ESR studies of the type reported here have been carried out on heterogeneous preparations of anti-dinitrophenyl antibodies, in the elegant pioneering studies of Stryer and Griffith [15], and Hsia and Piette [12]. Stryer and Griffith [15], using hapten spin label II, concluded that the dinitrophenyl binding site was a relatively rigid structure. Our results with spin label hapten V shows this even more clearly for the homogeneous antibody. Hsia and Piette [12] have used spin-labelled haptens of different lengths to probe the depth of the combining site by comparison with the spectra of a small isotropically tumbling nitroxide in solutions of different viscosities. They obtained a value of $10 \pm 1 \text{ \AA}$ for the longitudinal dimensions of the combining site, which is similar to the value obtained for the homogeneous antibody, in the present work. However, in cases of anisotropic motion which are undoubtedly found here this approach is inappropriate, as they pointed out. The present treatment based on analysis of the likely anisotropic motions, is to be preferred, and has the advantage of also yielding values for the transverse dimensions of the combining site.

It should be noted that the ESR spin label studies have shown unambiguously that the nitroxide moieties of spin labels I and V are almost completely immobilized in the antibody combining site. This is a pre-requisite for the quantitative assessment of the broadening effects observed in the NMR paramagnetic difference spectra in terms of distances of the various residues from the spin labelled hapten.

Finally we note the finding of lanthanide binding sites on the Fv fragment. This opens up the possibility of using the lanthanide-induced perturbation [8] in the NMR spectrum of the Fv fragment and the Fv-hapten complexes to obtain the spatial orientations of

the amino acid residues, in particular those in the region of the hapten combining site. Such experiments are currently being undertaken.

We wish to thank Professors R. R. Porter F.R.S., R. J. P. Williams F.R.S. and D. Givol for their encouragement and interest in this work. Professor D. Givol also generously sent us samples of the Fv fragment on which feasibility studies were carried out. We thank Dr M. Potter for sending us MOPC 315 tumor-bearing mice. Dr I. D. Campbell kindly supplied the data for Fig. 4. We also thank the Medical Research Council for their financial support. R.A.D. and A.I.W. are members of the Oxford Enzyme Group which is supported by the Science Research Council. D.M. is an I.C.I. Fellow. A.C.M. is a recipient of a postdoctoral fellowship from the Canadian Medical Research Council. We thank J.E.O.L. Co. Ltd. for the loan of an ESR spectrometer.

REFERENCES

- Campbell, I. D., Dobson, C. M., Williams, R. J. P. & Xavier, A. V. (1973) *Ann. N.Y. Acad. Sci.* **222**, 163–174.
- Inbar, D., Hochman, J. & Givol, D. (1972) *Proc. Natl Acad. Sci. U.S.A.* **69**, 2659–2662.
- Poljak, R. J., Amzel, L. M., Avey, H. P., Chen, B. L., Phizackerley, R. P. & Saul, F. (1973) *Proc. Natl Acad. Sci. U.S.A.* **70**, 3305–3310.
- Amzel, L. M., Poljak, R. J., Saul, F., Varga, J. M. & Richards, F. F. (1974) *Proc. Natl Acad. Sci. U.S.A.* **71**, 1427–1430.
- Schiffer, M., Girling, R. L., Ely, K. R. & Edmundson, A. B. (1973) *Biochemistry*, **12**, 4629–4631.
- Epp, O., Colman, P., Fehlhammer, H., Bode, W., Schiffer, M. & Huber, R. (1974) *Eur. J. Biochem.* **45**, 513–524.
- Padlan, E. A., Segal, D. M., Spande, T. F., Davies, D. R., Rudikoff, S. & Potter, M. (1973) *Nat. New Biol.* **245**, 165–167.
- Dwek, R. A. (1973) *Nuclear Magnetic Resonances in Biochemistry. Application to Enzyme Systems*, Clarendon Press, Oxford, England.
- Inbar, D., Rotman, M. & Givol, D. (1971) *J. Biol. Chem.* **246**, 6272–6275.
- Hochman, J., Inbar, D. & Givol, D. (1973) *Biochemistry*, **12**, 1130–1135.
- Porter, R. R. (1959) *Biochem. J.* **73**, 119–126.
- Hsia, J. C. & Piette, L. H. (1969) *Arch. Biochem. Biophys.* **129**, 296–307.
- Fraenkel-Conrat, H., Harris, J. I. & Levy, A. L. (1955) in *Methods of Biochemical Analysis* (Glick, D., ed.) vol. 2, pp. 359–425, Interscience, New York.
- Weiner, H. (1969) *Biochemistry*, **8**, 526–533.
- Stryer, L. & Griffith, O. H. (1965) *Proc. Natl Acad. Sci. U.S.A.* **54**, 1785–1791.
- Jones, R., Dwek, R. A. & Forsén, S. (1974) *Eur. J. Biochem.* **47**, 285–293.
- Myatt, R. W. (1974) D. Phil. Thesis, Oxford University, England.
- Smith, I. C. P., Marsh, D. & Schreier-Muccillo, S. in *Free Radicals in Biology* (Pryor, W. A., ed.) vol. 1, Academic Press, New York, in press.
- Griffith, O. H., Cornell, D. & McConnell, H. M. (1965) *J. Chem. Phys.* **43**, 2909–2910.
- Hubbell, W. L. & McConnell, H. M. (1971) *J. Am. Chem. Soc.* **93**, 314–326.

21. Brière, R., Lemaire, H. & Rassat, A. (1965) *Bull. Soc. Chim. Fr.* *11*, 3273–3283.
22. Campbell, I. D., Lindskog, S. & White, A. I. (1974) *J. Mol. Biol.* in press.
23. Campbell, I. D., Dobson, C. M., Williams, R. J. P. & Xavier, A. V. (1973) *J. Mag. Res.* *11*, 172–181.
24. Schreier-Muccillo, S., Marsh, D., Dugas, H., Schneider, H. & Smith, I. C. P. (1973) *Chem. Phys. Lipids*, *10*, 11–27.
25. Schulenburg Dugas, E., Bradshaw, R. A., Simms, E. S. & Eisen, H. N. (1973) *Biochemistry*, *12*, 5400–5416.
26. Francis, S. H., Leslie, R. G., Hood, L. & Eisen, H. N. (1974) *Proc. Natl Acad. Sci. U.S.A.* *71*, 1123.
27. Kabat, E. A. & Wu, T. T. (1971) *Ann. N.Y. Acad. Sci.* *190*, 382–393.
28. Haselkorn, D., Friedman, S., Givol, D. & Pecht, I. (1974) *Biochemistry*, *13*, 2210–2222.

R. A. Dwek, J. C. A. Knott, D. Marsh, A. C. McLaughlin, E. M. Press, N. C. Price, and A. I. White,
Department of Biochemistry, University of Oxford, South Parks Road, Oxford, Great Britain OX1 3QU